Model experiments and direct stability assessments on pure loss of stability of the ONR tumblehome in following seas

Jiang Lu, *China Ship Scientific Research Center,* lujiang1980@aliyun.com
Min Gu, *China Ship Scientific Research Center,* gumin702@163.com

ABSTRACT

The guidelines for direct stability assessment of pure loss of stability are currently under development at the International Maritime Organization (IMO) for the second generation intact stability criteria. A surge-heave-pitch-roll coupled equation named as 4 DOF is newly established for predicting pure loss of stability in following seas. Firstly, the thrust and the resistance of calm water are varied with the ship forward speed and the excited surge force by waves is varied with the relative position between the ship and waves. Secondly, the heave and pitch motions obtained by a strip method with an enhanced integrating method applied to an upright hull, in which the ship speed variation due to the surge motion is also newly considered, are used to determine the simultaneous relative position of the ship to waves in time domain, and then the nonlinear Froude-Krylov roll restoring variation is calculated by integrating the wave pressure up to the wave surface. Thirdly, the initial heeling angle, the nonlinear roll damping and the heel-induced hydrodynamic forces for large heeling angle in calm water are considered in the 4 DOF mathematical model, and the effect of the constant ship speed, the surge motion, the initial heeling angle, the heel-induced hydrodynamic forces and the heave and pitch motions on pure loss of stability are studied for direct assessment of pure loss of stability. Finally, the new numerical approach on pure loss of stability in following seas are verified by experimental results using the standard ONR tumblehome provided by an IMO's intercessional corresponding group.

Keywords: *Pure loss of stability, IMO, second generation intact stability criteria, direct stability assessment, surge-heave-roll-pitch.*

1. INTRODUCTION

The guidelines for direct stability assessment of pure loss of stability are currently under development at the International Maritime Organization (IMO) for the second generation intact stability criteria (IMO SDC 4, 2017). As one of the problems related to the roll restoring force variation, pure loss of stability in following seas has been studied for many years (Umeda & Yamakoshi , 1986), which is a nonlinear phenomenon involving a large amplitude roll motion, or even capsizing when the crest of a large wave passes the midship section of a ship with a slightly higher speed than the ship speed and the state of stability loss at the crest exists long enough. It is urgently required to establish reliable guidelines for developing accurate but sufficiently simple methods to predict pure loss of stability in following seas

Pure loss of stability is a nonlinear phenomenon involving a large amplitude roll motion and it is still difficult to be predicted quantitatively. Hashimoto carried out experiments on pure loss of stability in following seas with one surge-roll coupled mathematical model (Hashimoto, 2009). Umeda firstly pointed out that it could be not really pure for pure loss of stability in astern seas (Kubo et al., 2012). Japan delegation (IMO SLF 55, 2013) noted that predicting pure loss of stability with their newly 4 degrees of freedom (DOF) mathematical model is more accurate than the 2 DOF mathematical model. An experiment with a fishing vessel was carried out for further study on pure loss of stability (Umeda et al., 2017).

For drafting guidelines for direct stability assessment, several crucial elements for predicting parametric roll were investigated with simulations and experiments by the authors (Lu et al., 2017). Several crucial elements for pure loss of stability were investigated with experiments and one established mathematical model which refers a

MMG standard method for ship maneuvering predictions and existing mathematical models for broaching (Lu & Gu., 2017; Lu et al., 2018).

The capsizing due to pure loss of stability happens at a high speed in following and astern seas. In that case, the encounter frequency is much lower than the natural frequencies of heave and pitch, and the coupling with heave and pitch motions is almost static (Matsuda & Umeda, 1997). The above methods for pure loss of stability and existing mathematical models for broaching (Umeda, 1999; Umeda & Hashimoto, 2002; Hashimoto et al., 2011; Umeda et al., 2016) are based on a static balance assumption for heave and pitch motions.

The large amplitude roll motion and capsizing due to pure loss of stability are related to seakeeping, maneuvering, thrust and resistance. Unfortunately, they are still separated at this stage and the improvement of predicting methods for pure loss of stability are limited by the development of seakeeping and maneuvering. The above existing mathematical models are apt to maneuvering mathematical models in which the maneuvering coefficients are difficult to be obtained accurately except for expensive experiments at this stage. Therefore it is urgent to obtain a unified method to predict pure loss of stability with a seakeeping mathematical model combined with some essential maneuvering coefficients. In the seakeeping field, strip methods can obtain reasonable heave and pitch motions in the frequency domain when the ship speed is not very high, such as Ordinary Strip Method (OSM), New Strip Method (NSM) and STF Method (STFM). For predicting added resistance, Kashiwagi (Kashiwagi, 1995; Kashiwagi et al, 2010) developed an enhanced unified theory from the unify theory (Newman, 1978) in which an enhanced integrating method of a direct line integral is developed to solve the velocity potential to replace the traditional collocation method.

For predicting the large amplitude roll motion during pure loss of stability in following seas, a more accurate mathematical model is newly established with a surge-heave-pitch-roll coupled equation in which heave and pitch motions at each constant forward speed are obtained by a strip method with an enhanced integrating method of direct line integral applied to an upright hull. The non-uniform forward speed due to the surge motion is also newly considered by an interpolation method. Then the effect of the constant speed, the surge motion, the initial heeling angle, the heel-induced hydrodynamic forces and the heave and pitch motions on pure loss of stability are studied. The new numerical approach on pure loss of stability in following seas are verified by experimental results using the standard ONR tumblehome hull form which is provided by an IMO's intersessional correspondance group as one of standard ships for developing the second generation intact stability criteria.

2. MATHEMATICAL MODEL

Coordinate systems

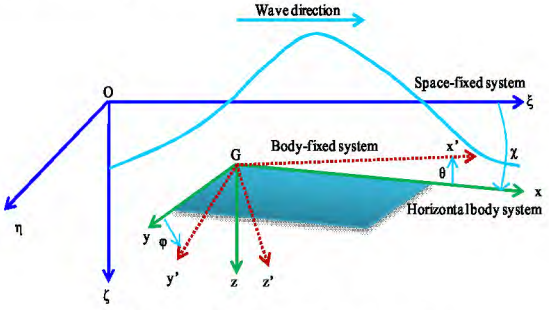

Figure 1: Coordinate systems

A space-fixed coordinate system $O-\xi\eta\zeta$ with the origin at a wave trough, a body-fixed system $G-x'y'z'$ with the origin at the center of gravity of the ship, and a horizontal body coordinate system $G-xyz$ (Hamamoto & Kim, 1993), which has the same origin with the body-fixed system but does not rotate around the x-axis and y-axis, are adopted as shown in Fig. 1.

The relationships between the horizontal body coordinate system $G-xyz$, the body-fixed system $G-x'y'z'$ and the space-fixed system $O-\xi\eta\zeta$ are shown in Eq. (1) and Eq. (2), respectively.

$$\begin{bmatrix} x \\ y \\ z \end{bmatrix} = \begin{bmatrix} \cos\theta & \sin\phi\sin\theta & \cos\phi\sin\theta \\ 0 & \cos\varphi & -\sin\varphi \\ -\sin\theta & \sin\varphi\cos\theta & \cos\varphi\cos\theta \end{bmatrix} \begin{bmatrix} x' \\ y' \\ z' \end{bmatrix} \quad (1)$$

$$\begin{bmatrix} \xi-\xi_G \\ \eta-\eta_G \\ \zeta-\zeta_G \end{bmatrix} = \begin{bmatrix} \cos\theta\cos\chi & \sin\varphi\sin\theta\cos\chi - \cos\varphi\sin\chi & \cos\varphi\sin\theta\cos\chi + \sin\varphi\sin\chi \\ \cos\theta\sin\chi & \sin\varphi\sin\theta\sin\chi + \cos\varphi\cos\chi & \cos\varphi\sin\theta\sin\chi - \sin\varphi\cos\chi \\ -\sin\theta & \sin\varphi\cos\theta & \cos\varphi\cos\theta \end{bmatrix} \begin{bmatrix} x' \\ y' \\ z' \end{bmatrix} \quad (2)$$

Mathematical Model

The 4 DOF mathematical model is expressed by surge, roll, heave and pitch motions as shown in Eq. (3) to Eq. (6), respectively. The time domain of ship positions in surge, heave and pitch are shown in Eq. (7), (8) and (9), respectively. The subscripts H, P and W refer to hull, propeller and wave, respectively.

$$(m + A_{11})\dot{u} = X_H + X_P + X_W \tag{3}$$

$$(I_{xx} + A_{44})\ddot{\varphi} = K_H - D(\dot{\varphi}) - W \cdot [GZ_W(\xi_G / \lambda, \zeta_G(t), \theta(t), \chi, \varphi) - GZ(\varphi)] \tag{4}$$

$$(m + A_{33}(u))\ddot{\zeta} + B_{33}(u)\dot{\zeta} + C_{33}\zeta + A_{35}(u)\ddot{\theta} + B_{35}(u)\dot{\theta} + C_{35}\theta = F_3^{FK}(u) + F_3^{DF}(u) \tag{5}$$

$$(I_{yy} + A_{55}(u))\ddot{\theta} + B_{55}(u)\dot{\theta} + C_{55}\theta + A_{53}(u)\ddot{\zeta} + B_{53}(u)\dot{\zeta} + B_{53}\zeta = F_5^{FK}(u) + F_5^{DF}(u) \tag{6}$$

$$\xi_G = \int\int_0^t \dot{u}(t)dtdt \tag{7}$$

$$\zeta_G(t) = \zeta_{Ga}(u)\cos(\omega t - k\xi_G \cos\chi + \delta_H(u)) \tag{8}$$

$$\theta(t) = \theta_a(u)\cos(\omega t - k\xi_G \cos\chi + \delta_\theta(u)) \tag{9}$$

where m: ship mass; u: surge velocity; X_H, K_H: surge force and roll moment around center of ship gravity acting on ship hull; X_P: surge force due to propeller; X_W: surge force due to waves; I_{xx}, I_{yy}: moment of inertia in roll and pitch; φ: roll angle; $D(\dot{\varphi})$: roll damping moment; W: ship weight; GZ_W: righting arm in waves; GZ: righting arm in calm water; t: time; $\zeta_G(t)$: heave displacement; $\theta(t)$: pitch angle, ξ_G: instantaneous ship longitudinal position; λ: wave length; χ: heading angle; F_3^{FK}, F_3^{DF}: wave exciting force on heave direction including Froud-Krylov component and diffraction component. F_5^{FK}, F_5^{DF}: wave exciting moment on pitch direction including Froud-Krylov component and diffraction component. $\zeta_{Ga}(u)$, $\delta_H(u)$: amplitude and initial phase of heaving when the ship forward speed is u; $\theta a(u)$, $\delta_\theta(u)$: amplitude and initial phase of pitching when the ship forward speed is u; ω: wave frequency; k: wave number; The dot denotes the differentiation with time. A_{ij}, B_{ij}, C_{ij} are coupling coefficients, and 1,3,4,5 denote the direction in surge, heave, roll and pitch, respectively.

Hydrodynamic forces acting on a ship

The hull forces in still water X_H and K_H are expressed as follows:

$$X_H = -R(u) \tag{10}$$

$$K_H = \frac{1}{2}\rho L_{pp} d^2 u^2 K'_\varphi \cdot \varphi \tag{11}$$

where, $R(u)$: ship resistance in calm water; ρ: water density; d: ship draft; K'_φ: the non-dimensional derivative for roll moment with respect to roll angle.

Propeller thrust and the hull resistance in still water

The surge force due to propeller thrust X_P with twin propellers is expressed as follows.

$$X_P = 2 \times (1 - t_P)T \tag{12}$$

$$T = \rho n_P{}^2 D_P^4 K_T(J_P) \tag{13}$$

$$J_P = \frac{(1 - w_P)\,u}{n_P D_P} \tag{14}$$

The hull resistance in still water R in the surge motion is expressed as follows:

$$R = \frac{1}{2}\rho S_F u^2 C_T\left(\frac{u}{\sqrt{gL_{PP}}}\right) \tag{15}$$

where, t_P: thrust deduction factor; T: propeller thrust; n_P: propeller revolution number; D_P: propeller diameter; K_T: thrust coefficient of propeller; J_P: propeller advanced ratio; w_P: wake fraction at propeller position; S_F: wetted hull surface area; C_T: total resistance coefficient in calm water; g: gravitational acceleration.

Initial values for numerical integration with time are set as follows:

$$t = 0\,; \xi_G = 0, u = 0, n = n^* \tag{16}$$

where, n^*: denotes the desired propeller revolution rate.

Excited surge force by waves

The wave-induced forces as the sum of the Froude-Krylov force (W_FK) and the diffraction force (W_Dif) including hydrodynamic lift forces acting on the hull are used for broaching by Umeda and Hashimoto (Umeda & Hashimoto, 2002), and only Froude-Krylov force in the surge direction is considered and it is expressed as follow.

$$X_W(\xi_G / \lambda, u, \chi) = X_{W\_FK}(\xi_G / \lambda, u, \chi) = -\rho g \zeta_w k \cos\chi \cdot \int_{AE}^{FE} C_1(x)S(x)e^{-kd(x)/2}\sin k(\xi_G + x\cos\chi)dx \tag{17}$$

$$C_1 = \frac{\sin(k \sin\chi \cdot B(x)/2)}{k \sin\chi \cdot B(x)/2} \quad (18)$$

where, *AE, FE*: after section and forward section; ζ_w: amplitude of incident waves; *B(x)*: sectional breadth; *S(x)*: sectional area.

Roll restoring force variation

Pure loss of stability is one of the problems related to the roll restoring force variation. The restoring force variation can be calculated by integrating the pressure around the instantaneously wetted hull surface with static balance of heave and pitch which is based on a Froude-Krylov assumption (Hamamoto & Kim, 1993) and it is widely used to predict parametric roll using heave and pitch motions obtained by Ordinary Strip Method (Lu et al., 2017). Here non-uniform forward speed due to the surge motion in following seas is further considered. As a result, the following formula is used.

$$\begin{aligned} W \cdot GZ_{FK} &= \rho g \int_L y(x, X_G, t) \cdot A(x, \xi_G, t)\, dx \\ &+ \rho g \sin\chi \cdot \int_L z(x, \xi_G, t) \cdot F(x) \cdot A(x, \xi_G, t) \\ &\cdot \sin(\xi_{G0} + (X_G + x)\cos\chi - c \cdot t) dx \end{aligned} \quad (19)$$

$$F(x) = \zeta_w\, k \frac{\sin(k\frac{B(x)}{2}\sin\chi)}{k\frac{B(x)}{2}\sin\chi} e^{-k\,d(x)} \quad (20)$$

where, $A(x,\xi_G,t)$: the submerged area of local section of the ship; $y(x,\xi_G,t)$: the transverse position of buoyancy centre of local section; $z(x,\xi_G,t)$: the vertical position of buoyancy centre of local section; ξ_{G0}=0: the initial longitudinal position of a ship centre from a wave trough.

Heave and pitch motions

The large amplitude roll motion and capsizing due to pure loss of stability are related to low encounter frequency of heave and pitch motions. For finding a method to obtain stable heave and pitch motions in following seas at a high speed, firstly, the authors calculated heave and pitch motions with Ordinary Strip Method (OSM) using the collocation method to solve the velocity potential and a strip method using an enhanced integrating method of direct line integral (Kashiwagi et al., 2010) to solve the velocity potential named as EStrip in this paper for the modified Wigley model (Kashiwagi et al., 2010) in head seas. Then the calculated results are compared with the model experiments published by Kashiwagi and their results of Enhanced Unified Theory (EUT) (Kashiwagi et al., 2010) as shown in Figs. A1-A2. Both OSM and EStrip methods show reasonably good agreement in heave and pitch motions in head seas at low speeds. The heave and pitch motions calculated by OSM and EStrip methods are further compared in head seas at high speed as show in Fig. A3. Both OSM and EStrip methods can generate stable heave and pitch motions at Fn=0.4. For obtaining stable heave and pitch motions for pure loss of stability, the heave and pitch motions in following seas with OSM and EStrip methods are further investigated as shown in Figs. A4-A5. Both OSM and EStrip methods could generate the same results at a low speed, but the pitch motion calculated by the EStrip method is more stable than that calculated by the OSM method at a high speed. Since pure loss of stability could happen at a high speed in following seas, the EStrip method is used to calculate heave and pitch motions at each constant forward speed applied to an upright hull while non-uniform forward speed is considered by an interpolation method in this paper.

Roll damping force

Roll damping is one of essential terms for predicting roll motion, especialy large amplitude roll motions. Linear and cubic nonlinear roll damping coefficients are used for predicting parametric roll and linear and squared nonlinear roll damping coefficients are used for predicting dead ship stability in the vulnerability criteria (IMO SDC 4, 2017). Linear and cubic nonlinear roll damping coefficients are adopted as shown in Eq.(21) for predicting pure loss of stability.

$$D(p) = (I_{xx} + J_{xx})(\alpha \cdot p + \gamma \cdot p^3) \quad (21)$$

3. EXPERIMENTS

The free running experiment with a 1/40.526 scaled model of the ONR tumblehome vessel was conducted in the seakeeping basin (length: 69m, breadth: 46m, depth: 4m) of China Ship Scientific Research Center, which is equipped with flap wave makers at the two adjacent sides of the basin.

The ship model was driven by twin propellers in regular following seas in the free running experiment. The roll angle, pitch angle and yaw angle were measured by the MEMS (Micro Electro-Mechanical System)-based gyroscope placed on the

ship model and the roll angle, pitch angle, yaw angle, rudder angle and propeller rate were recorded by an on-board system which is connected with an on-shore control computer by a wireless connection. The wave elevation was measured at the middle position of the basin by a servo-needle wave height sensor attached to a steel bridge which is 78m in length and spans over the basin.

Roll damping is very important for predicting large amplitude roll motions and even capsizing due to pure loss of stability, and here free roll decay tests in calm water are conducted to obtain roll damping coefficients. The speed is a key factor for pure loss of stability, and here the nominal Froude number (Fn) is used for the experiment of pure loss of stability in following seas by using the same specified propeller rate in calm water. The specified propeller rate corresponding to one nominal speed in calm water is determined by measuring instantaneous position of the model ship with a total station system, and the total station system consists of a theodolite and a prism attached to the model ship as shown in Fig.2.

First the model is kept near the wave maker by hands of two workmen sitting on the carriage and the initial heading of the model is kept referring to the steel bridge which can rotate about its center, up to 45 degree. Next, the wave-making system starts to generate waves. Then the propeller revolutions increase up to specified value after receiving the order from the on-shore control computer. When the wave train propagates far enough, the model is released free near one wave crest with its initial heading, and then the model automatically runs in following or quartering seas with its specified propeller rate and auto pilot course.

Figure 2: The theodolite and the prism attached on the model ship

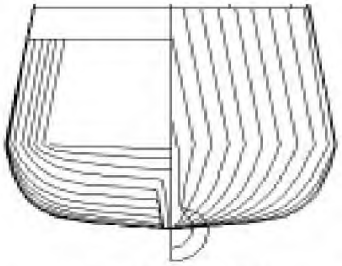

Figure 3: The ONR Tumblehome lines

The subject ship is the ONR Tumblehome vessel. The principal particulars and the lines of the ONR Tumblehome vessel are shown in Table 1 and Fig. 3, respectively. The ship model in the free running experiment is shown in Fig. 4.

Table 1: Principal particulars of the ONR tumblehome

Items	Ship	Model
Length: L	154.0 m	3.8 m
Draft: d	5.494m	0.136 m
Breadth: B	18.8 m	0.463 m
Depth: D	14.5 m	0.358 m
Displ.: W	8507 ton	0.1278 ton
C_b	0.535	0.535
GM	1.48 m	0.037 m
OG	-2.729 m	-0.067 m
L_{CB}	-2.569 m	-0.063 m
T_φ	14.0 s	2.199 s
κ_{yy}	0.25 L	0.25 L
K_{zz}	0.25 L	0.25 L
$2\times A_R$	2×23.74m^2	2×0.0145 m^2
D_P	5.22m	0.129m
δ_{max}	35degs	35degs

Figure 4: The ship model in the free running experiment

4. RESULTS AND DISCUSSIONS

The effect of speed on the heave and pitch motions

Pure loss of stability could happen in following seas at a high speed, and it is related to seakeeping problems of the high speed and low encounter frequency. The methods for pure loss of stability mostly are based on a static balance assumption for heave and pitch motions. As discussed in paragraph 2.7 and the appendix, one strip method with an enhanced integrating method of a direct line integral for solving the velocity potential is used to calculate heave and pitch motions at each constant forward speed applied to an upright hull. Then the non-uniform forward speed due to the surge motions is considered by an interpolation method in this paper. Here the effect of forward speed on the heave and pitch motions for the ONR tumblehome ship is further investigated. As shown in Fig. 5, the amplitude and initial phase of heave motions obtained by the EStrip method at zero forward speed are almost the same as that obtained by the static method and the OSM method, while small differences exist with increasing forward speeds.

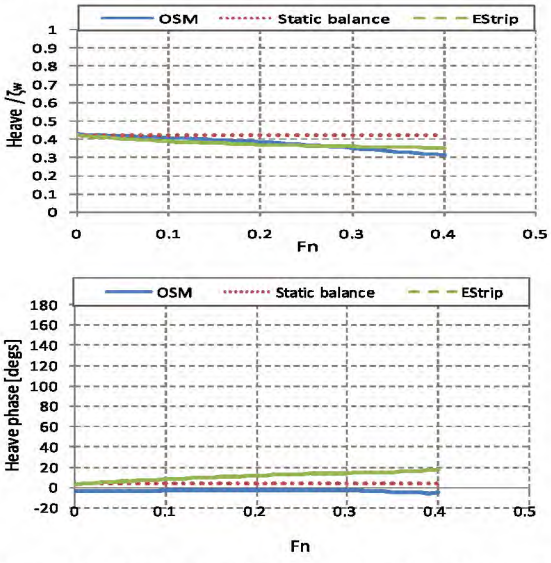

Figure 5: Heaving motion as a function of the Froude number in following seas with φ=0^0 and λ/Lpp=1.25.

As shown in Fig. 6, the amplitude and initial phase of pitch motions obtained by the EStrip method at zero forward speed are almost the same as that obtained by the static method and the OSM method, while the amplitude of pitch motions obtained by the OSM method obviously becomes small with increasing forward speeds. The critical Froude number of pure loss of stability is much smaller than 0.4, and the heave and pitch motions obtained by the Estrip method can be used to predict pure loss of stability for the ONR tumblehome vessel.

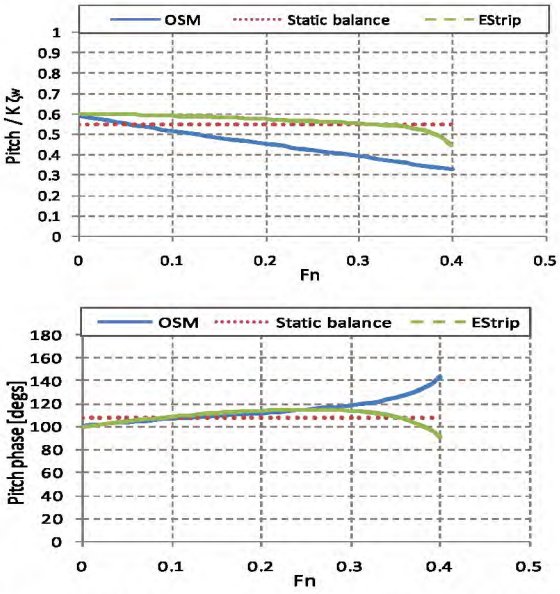

Figure 6: Pitching motion as a function of the Froude number in following seas with φ=0^0 and λ/Lpp=1.25.

The effect of wave on roll restoring variation

When the midship section is located on the crest in following seas, the metacentric height is reduced and may be negative. The righting arm in calm water GZ, the restoring variations in waves with static balance method GZ_W-static and with the strip method at different constant forward speeds GZ_W(Fn=0.0/0.1/0.2/0.3) are shown in Fig. 7. The stability loss at the crest is heavy, and if the state of stability loss at the crest exists long enough, capsizing could happen.

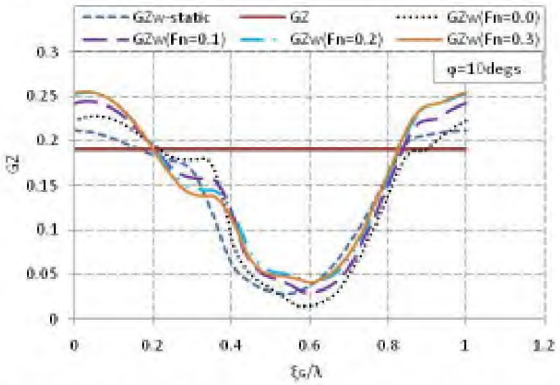

Figure 7: Restoring variation in following seas with φ=10^0 , λ/Lpp=1.25, H/Lpp=0.05, and χ=0^0

The effect of constant speed on pure loss of stability

The righting arm in calm water GZ and the restoring variations in waves GZ_W at different constant forward speed are shown in Fig. 8. The

encounter period becomes larger as the ship increasing forward speed, and the state of stability loss at the wave crest becomes larger.

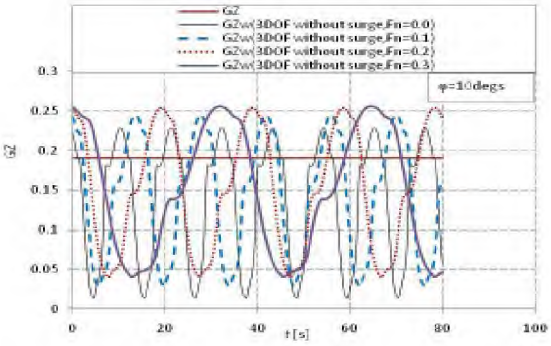

Figure 8: Time domain restoring variation in following seas with φ=10⁰, *λ/Lpp*=1.25, *H/Lpp*=0.05, and χ=0⁰.

The roll angle due to pure loss of stability at different constant forward speeds are shown in Fig. 9, and the roll angle becomes larger as the ship forward speed increases because the state of stability loss at crest becomes larger as shown in Fig. 8. But the state of stability loss at crest is not long enough to result in capsizing.

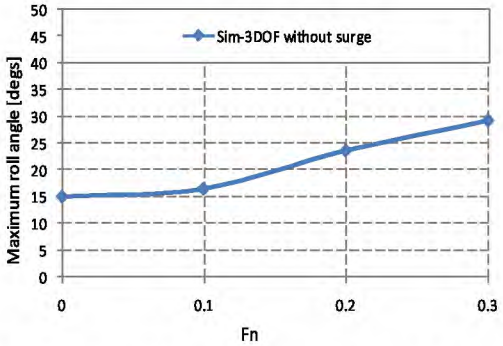

Figure 9: The effect of the constant speed on pure loss of stability with an initial heeling φ=8.6°, *λ/Lpp*=1.25, *H/Lpp*=0.05, and χ=0°.

The effect of surge motion on pure loss of stability

The nominal velocity of ship with Fn=0.3, the actual velocity of ship and the wave velocity are shown in Fig. 10. The nominal velocity of ship is much smaller than the wave velocity, and the maximum actual velocity of ship is also smaller than the wave velocity. The forward speed is varied in a large range around the nominal speed of ship due to the surge motion, and the state at the crest exists longer than that at the trough.

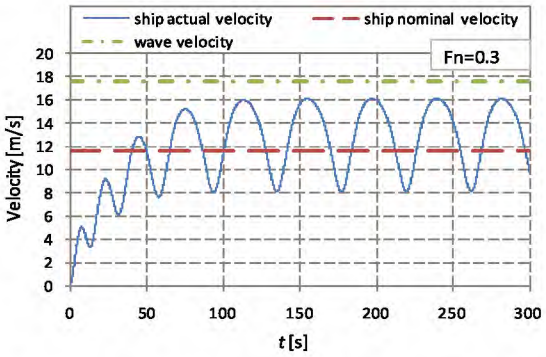

Figure 10: Comparison between ship velocity and wave velocity with nominal *Fn*=0.3, *λ/Lpp*=1.25, *H/Lpp*=0.05, and χ=0⁰.

The righting arm in calm water GZ, the restoring variations in waves GZ_W with surge and without surge are shown in Fig. 11. The state of stability loss at the crest exists longer than that at the trough because the surge motion causes the state at the crest to exist longer than that at the trough as shown in Fig. 10.

As shown in Fig. 12, the mathematical model with 3 DOF of heave-roll-pitch coupled motions fails to predict capsizing because the state of stability loss at the crest is not long enough while that with 4 DOF of surge-heave-roll-pitch coupled motions could appropriately estimate the pure loss of stability in following seas. One key reason is that the state at the crest exists longer than that at the trough due to the surge motion and then the state of stability loss at the crest exists long enough. Therefore, the surge motion is important for predicting pure loss of stability in following seas.

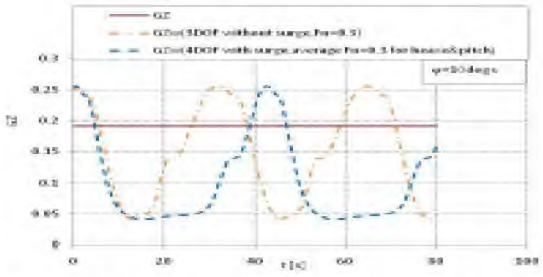

Figure 11: The effect of surge motion on restoring variation with φ=10°, *λ/Lpp*=1.25, *H/Lpp*=0.05, and χ=0°.

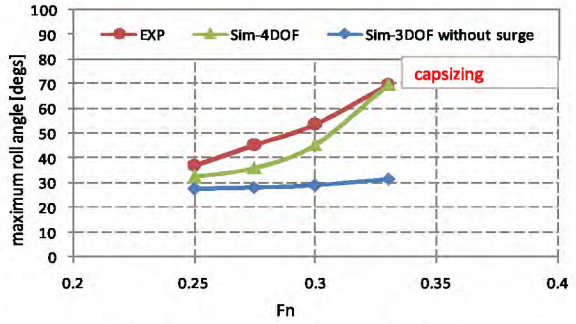

Figure 12: The effect of the sure motion on pure loss of stability with an initial heeling φ=8.6 , *λ/Lpp*=1.25, *H/Lpp*=0.05 and χ=0°.

The effect of initial heel angle on pure loss of stability

Without an external heeling moment, once the wave crest passes the ship, the ship will finally return to the upright position with regained stability in following seas as shown in Fig. 13 with $\varphi=0^0$. The initial heeling angle is set as 8.6 degrees by cargo shift in the experiment and capsizing happens due to pure loss of stability as shown in Fig.12. For investigating the effect of initial heeling angle on pure loss of stability, simulations with different initial heeling angles are carried out as shown in Fig. 13. The roll angles become larger as the initial heeling angles increases, and capsizing happens at the critical speeds due to pure loss of stability. However, the ship could be captured by a wave crest when the ship has a very small initial heeling angle in following seas at a high speed. That is to say, the ship reaches the speed of the wave in this case.

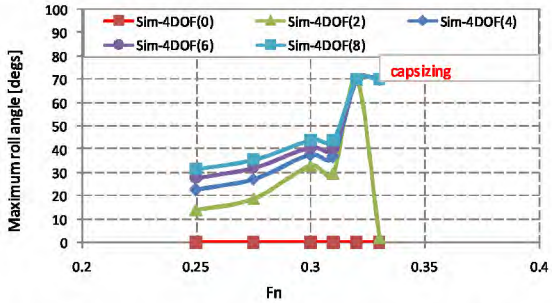

Figure 13: The effect of initial heeling angles on pure loss of stability with *λ/Lpp*=1.25, *H/Lpp*=0.05, and χ=0° (φ=0°, φ=2°, φ=4°, φ=6°, φ=8°)

The effect of heel-induced hydrodynamic forces for large heeling angle in calm water

Pure loss of stability is accompanied with large amplitude roll motions. The heel-induced hydrodynamic forces for large heeling angle in calm water, which are hydrodynamic lift due to underwater non-symmetry induced by heeling angle with the forward velocity, could affect the prediction of pure loss of stability.

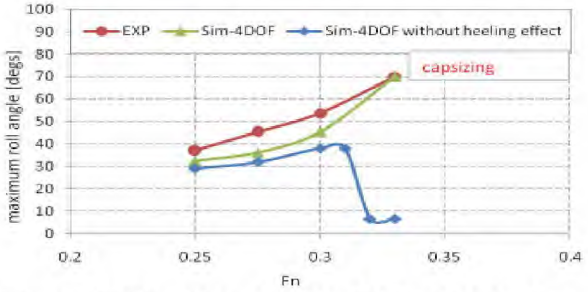

Figure 14: The effect of the heel-induced hydrodynamic forces on pure loss of stability with an initial heeling φ=8.6, *λ/Lpp*=1.25, *H/Lpp*=0.05 and χ=0°.

The linear heel-induced hydrodynamic forces in calm water are investigated as shown in Fig. 14. The 4 DOF mathematical model without linear heel-induced hydrodynamic forces could fail to predict capsizing at critical ship speeds due to pure loss of stability.

The effect of heave and pitch motions on pure loss of stability

The non-uniform forward speed due to the surge motion is newly considered for the heave and pitch motions in the surge-heave-pitch-roll coupled 4 DOF mathematical model for predicting pure loss of stability. The righting arm in calm water GZ, the restoring variations in waves GZ_W with the uniform and non-uniform forward speeds for the heave and pitch motions are shown in Fig. 15 and the predictions of pure loss of stability are shown in Fig. 16.

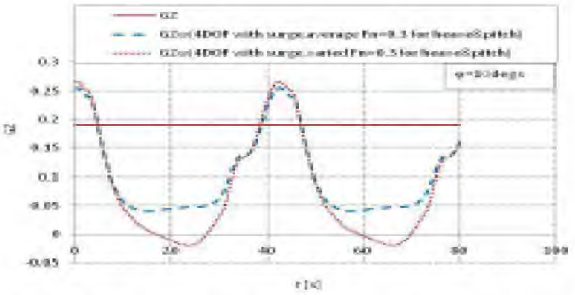

Figure 15: The effect of heave and pitch motions on restoring variation with φ=10°, *λ/Lpp*=1.25, *H/Lpp*=0.05 and χ=0°.

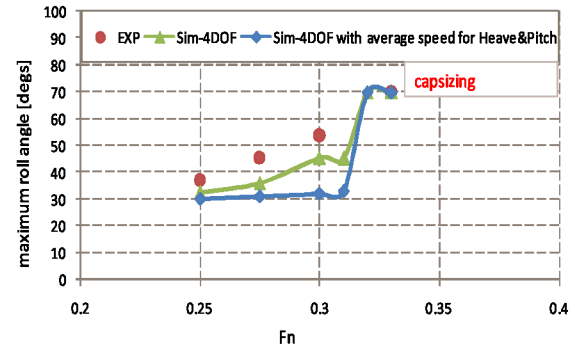

Figure 16: The effect of heave and pitch motions on pure loss of stability with φ=8.6°, λ/Lpp=1.25, H/Lpp=0.05 and χ=0°.

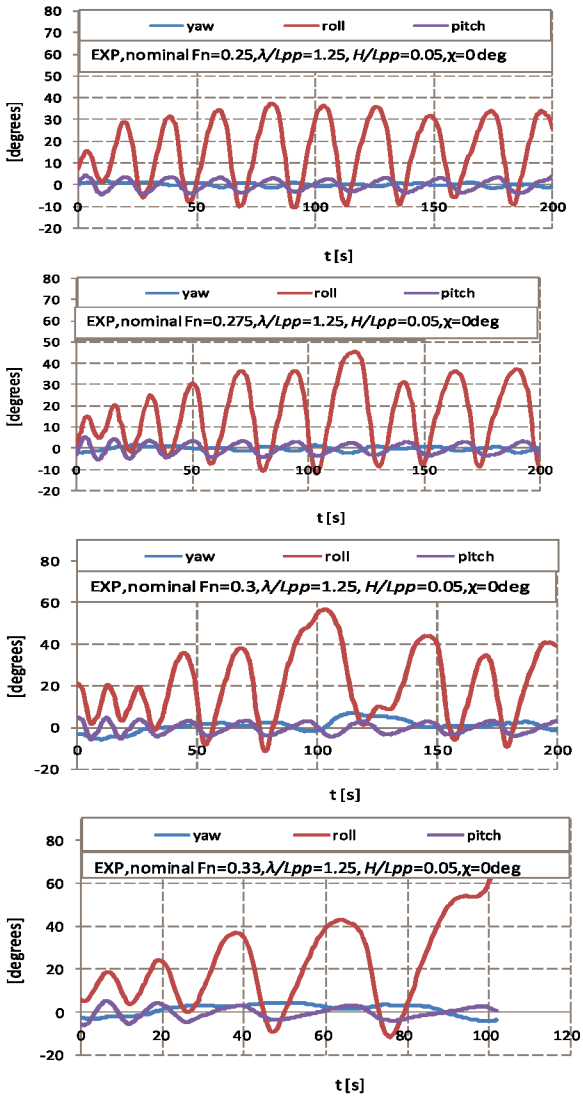

Figure 17: Yaw, roll and pitch motions in the free running experiment with an initial heeling φ=8.6°, λ/Lpp=1.25, H/Lpp=0.05 and χ=0°.

The method considering uniform forward speeds for the heave and pitch motions can predict capsizing due to pure loss of stability at the critical forward speed, but it could underestimate the roll angles at speeds below the critical forward speed. This because the stability loss at the crest with the non-uniform forward speed for the heave and pitch motions are larger than that with the uniform forward speed for the heave and pitch motions, as shown in Fig. 15.

The type of roll motions during pure loss of stability

The experimental results of yaw, roll and pitch motions in following seas are shown in Fig. 17. The roll motions become unstable when she ship speed near the critical speed of pure loss of stability. The capsizing happens due to pure loss of stability when the ship speed reaches the critical speed as shown in Fig. 17.

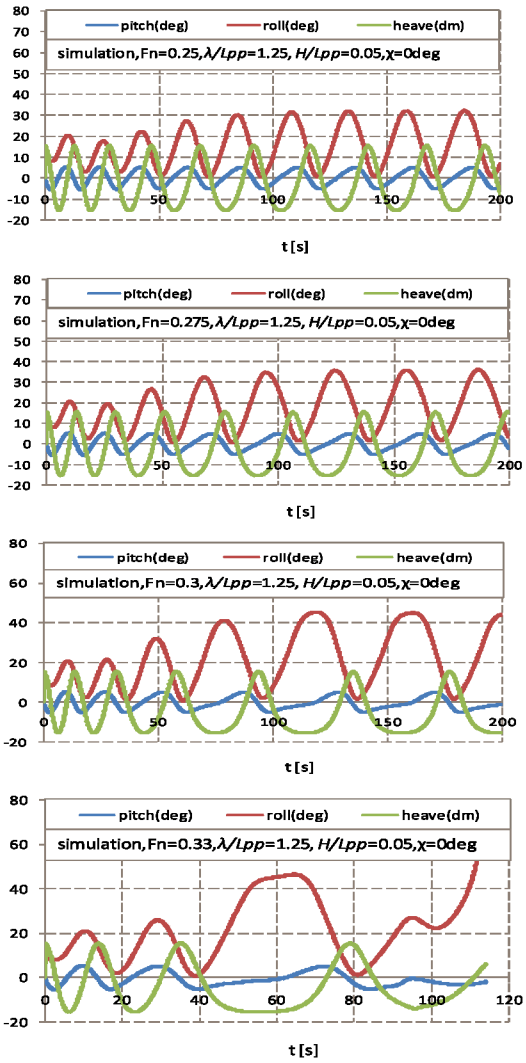

Figure 18: Pitch, roll and heave motions in the simulations with the 4 DOF mathematical model with an initial heeling φ=8.6°, λ/Lpp=1.25, H/Lpp=0.05 and χ=0°.

The calculated results of pitch, roll and heave motions in following seas with the 4 DOF mathematical model are shown in Fig. 18. The roll motions become large with the ship speed increasing,

and capsizing happens due to pure loss of stability when the ship speed reaches the critical speed. The roll amplitudes are agreed well with the experimental results, while the unstable roll motions cannot be completely repeated in the simulations. Pure loss of stability is more complicated than our previous understanding, although the roll angle and capsizing due to pure loss of stability can be predicted.

5. CONCLUSIONS

On the basis of the new numerical approach on pure loss of stability in following seas with one experiment by using the ONR tumblehome vessel, the following remarks can be made:

1) The new numerical approach with surge- -heave-pitch-roll coupled 4 DOF mathematical model considering the non-uniform forward speed for the heave and pitch motions obtained by a strip method with an enhanced integrating method applied to an upright hull could appropriately estimate pure loss of stability in following seas.
2) The encounter period becomes larger with increasing forward speed, while the surge motion further extends the state of stability loss at the crest. The effect of surge motion with varied forward speed on pure loss of stability in following seas should be considered.
3) The effect of linear heel-induced hydrodynamic forces in calm water on pure loss of stability in following seas should be taken into account for the ONR tumblehome vessel.

A unified method to predict pure loss of stability in astern waves with a seakeeping mathematical model combined with some essential maneuvering coefficients will be further investigated in future.

ACKNOWLEDGMENTS

Some contents used in this research were once guided by Prof. Naoya Umeda during the first author's Ph.D course at Osaka University supported by China Scholarship Council [No.2008606031]. Prof. M. Kashiwagi from Osaka University once provided the first author with his useful lecture and textbook on enhanced unified theory. The research is supported by Ministry of Industry and Information Technology of China (No. [2016] 25, 26; [2017] 614) and China research fund (No. B2420132001; No. 51509124). These supports are gratefully acknowledged.

REFERENCES

Hamamoto M., Kim Y.S., 1993, "A New Coordinate System and the Equations Describing Manovering Motion of a Ship in Waves", *Journal of the Society of Naval Architects of Japan*, 173: 209-220.

Hashimoto H., 2009, "Pure Loss of Stability of a Tumblehome Hull in Following Seas", Proceedings of the 19th International Offshore and Polar Engineering Conference Osaka, Japan, June 21-26.

Hashimoto H., Umeda N., Matsuda A., 2011, "Broaching Prediction of a Wave-piercing Tumblehome Vessel with Twin screws and Twin Rudders", *Journal of Marine Science and Technology*, 16:448-461.

IMO SLF 55, 2013, "Development of Second Generation Intact Stability Criteria", INF. 15. Annex 12

IMO SDC 2017, "Finalization Second Generation Intact Stability Criteria", Report of the working group, SDC 4/WP4.

Kashiwagi M, 1995, "Prediction of Surge and Its Effect on Added Resistance by Means of the Enhanced Unified Theory", *Trans. West-Japan Society of Naval Architects*, 89:77-89.

Kashiwagi M., Ikeda T. Sasagawa T., 2010, "Effect of Forward Speed of a ship on Added Resistance in waves", *International Journal of Offshore and Polar Engineering*, 20(2):1 -8.

Kubo H., Umeda N., Yamane K., Matsuda A., 2012, "Pure Loss of Stability in Astern Seas -Is It Really Pure?", Proceedings of the 6th Asia-Pacific Workshop on Marine Hydrodynamics, pp. 307-312.

Lu J., Gu M., Umeda N., 2017, "Experimental and Numerical Study on Several Crucial Elements for Predicting Parametric Roll in Regular Head Seas", *Journal of Marine Science and Technology*, 22:25-37.

Lu J., Gu M., 2017, "Study on Standard Mathematical Model of Pure Loss of Stability in Stern-quartering Waves", Proceedings of the 16th International Ship Stability Workshop, Belgrade, Serbia, pp. 181-190.

Lu J., Gu M., Wang T., Chao S., 2018, "Experimental and Numerical Study on Standard Mathematical Model of Pure Loss of Stability", Proceedings of the 14th International Conference on Stability of Ships and Ocean Vehicles, (STAB2018), Kobe, Japan, pp. 164-178.

Matsuda A., Umeda N., 1997, "Vertical Motions of a Ship Running in Following and Quartering Seas", *Naval Architecture and Ocean Eng.* 227:47-55 (in Japanese).

Newman J. N., 1978, "The theory of ship motions", *Advances in Applied Mechanics*, 18:221-83

Umeda N. and Yamakoshi Y., 1986, "Experimental study on Pure Loss of Stability in Regular and Irregular Following Seas", Proc. of the 3rd International Conf. on Stability of Ships and Ocean Vehicles, (STAB1986), pp. 93-99.

Umeda N., 1999, "Nonlinear Dynamics of Ship Capsizing due to Broaching in Following and Quartering Seas", *Journal of Marine Science and Technology*, 4:16-26.

Umeda N. and Hashimoto H., 2002, "Qualitative Aspects of Nonlinear Ship Motions in Following and Quartering Seas with High Forward Velocity", *Journal of Marine Science and Technology*, 6:111-121.

Umeda N., Usada S., Mizumoto K., Matsuda A, 2016, "Broaching Probability for a Ship in Irregular Stern-quartering Waves: Theoretical Prediction and Experimental Validation", *Journal of Marine Sci. and Techn.*, 21:23-37.

Umeda N., Osugi M., Sakai M., Matsuda A., Terada D., 2017, "Model Experiment on Pure Loss of Stability for a Ship in Astern Waves and Its Relationship with the Second Generation Intact Stability Criteria", Proceedings of the 16th International Ship Stability Workshop, Belgrade, Serbia, pp. 21-26.

APPENDIX: VALIDATION OF THE CALCULATION OF HEAVE AND PITCH MOTIONS WITH DIFFERENT METHODS

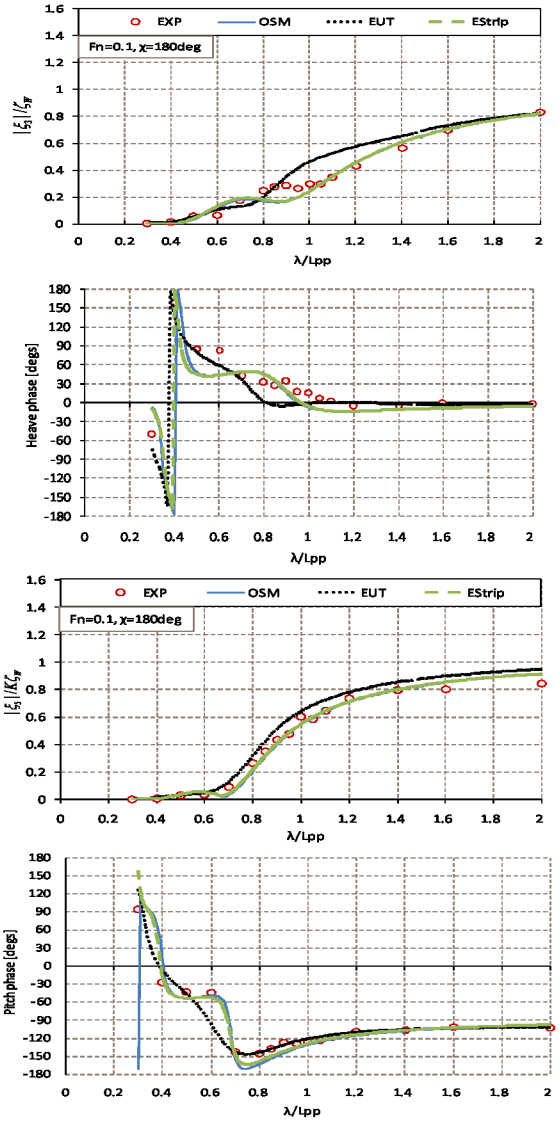

Figure A1: Heave and pitch motions of the modified Wigley ship model with different methods and experimental (EXP) and theoretical (EUT) results by Kashiwagi et al.(2010) at Fn=0.1 in head seas.

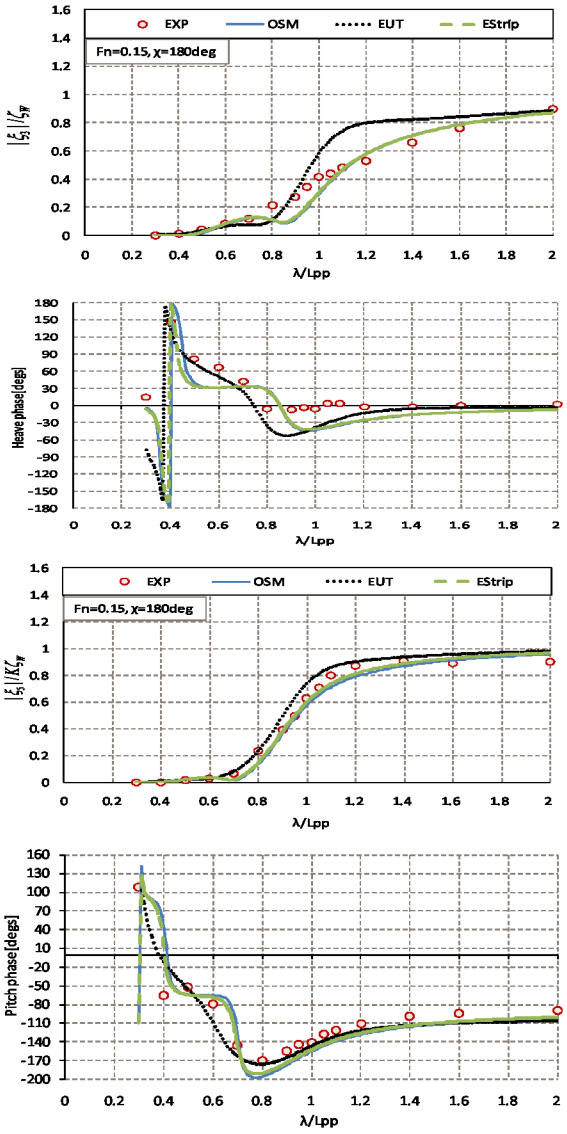

Figure A2: Heave and pitch motions of the modified Wigley ship model with different methods and experimental (EXP) and theoretical (EUT) results by Kashiwagi et al. (2010) at Fn=0.15 in head seas.

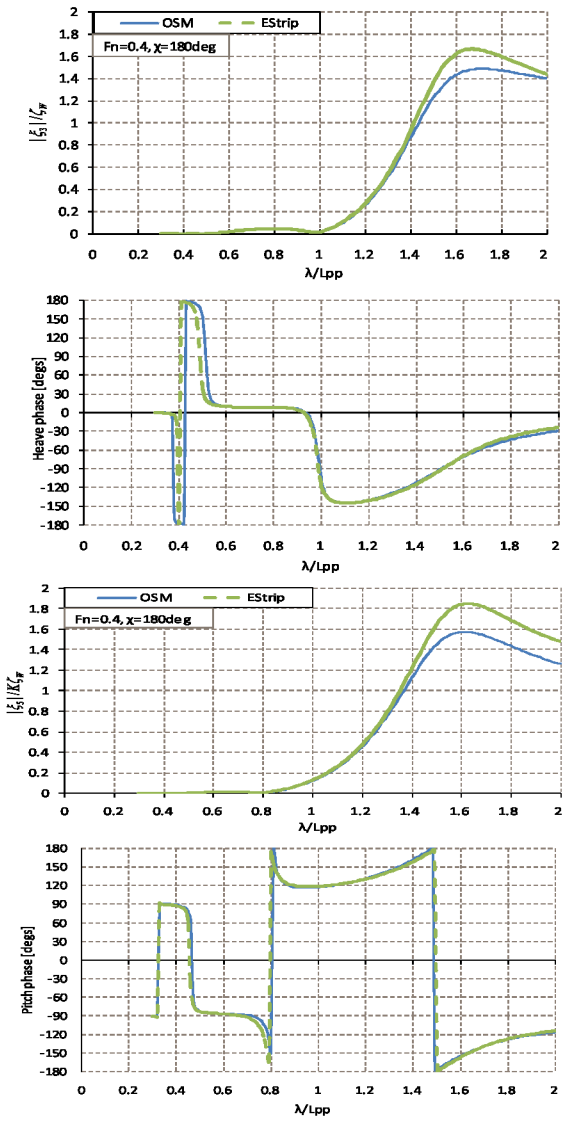

Figure A3: Heave and pitch motions of the modified Wigley ship model with different methods at Fn=0.4 in head seas.

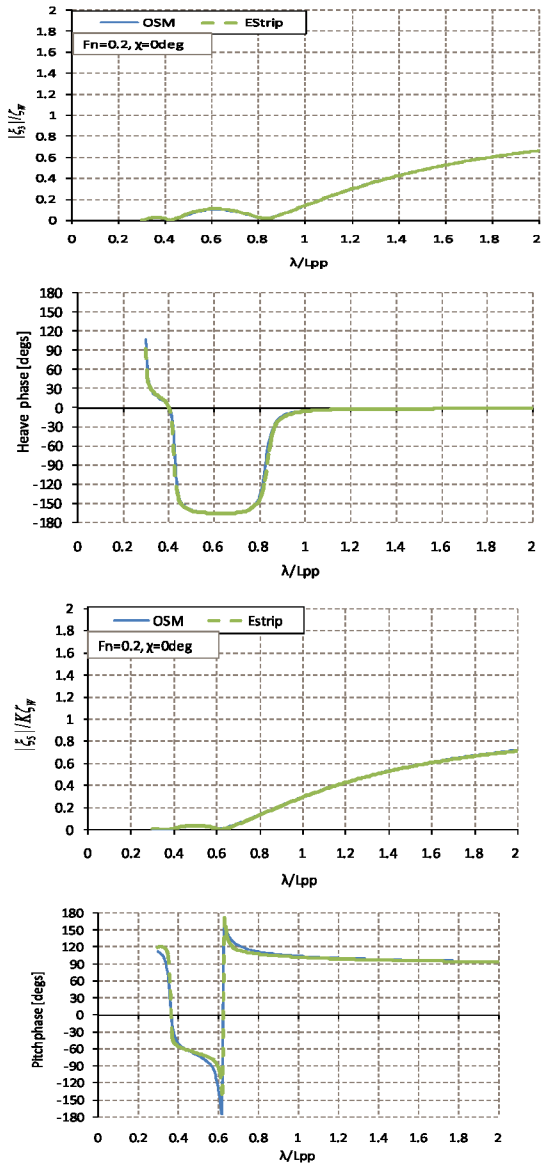

Figure A4: Heave and pitch motions of the modified Wigley ship model with different methods at Fn=0.2 in following seas.

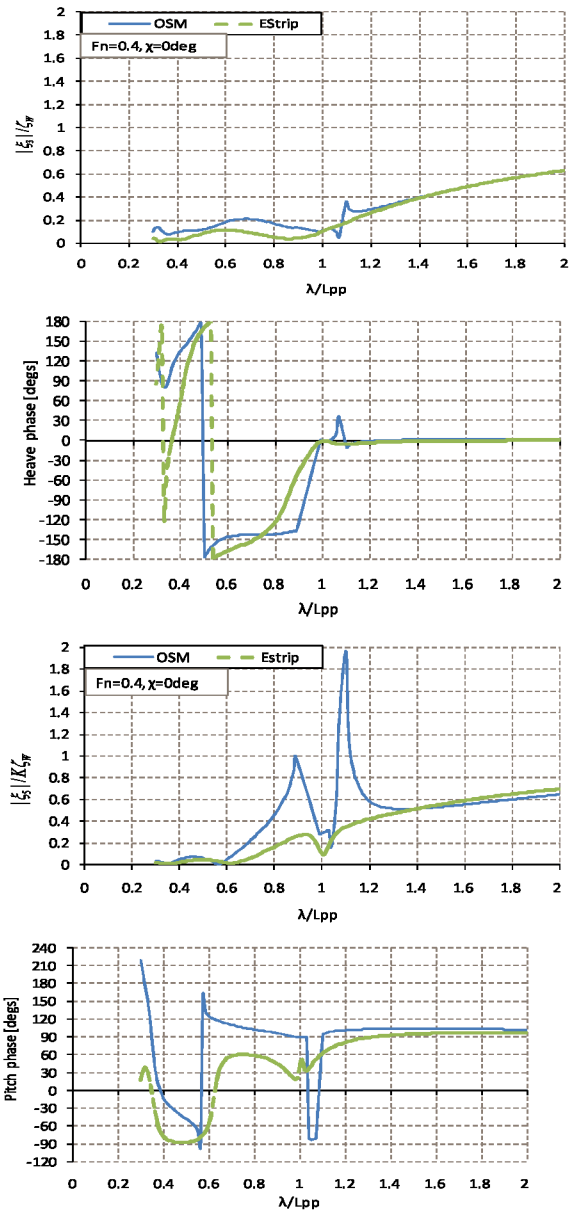

Figure A5: Heave and pitch motions of the modified Wigley ship model with different methods at Fn=0.4 in following seas.